Fatigue Evaluation of Offshore Wind Turbines Using In-Situ Strain Data

HOU QIAO, GUANGMING XU, CE SHEN, YONGLEI SU, WEI LI and CHUANRUI GUO

ABSTRACT

The development of offshore wind power has increased rapidly in recent years due to its clean and renewable nature. However, the design of offshore wind turbines is difficult and costly. As a result, the development cost remains high. Among them, fatigue of the steel structures in offshore wind turbine foundations is one of the most severe structural diseases, significantly affecting offshore wind development and maintenance costs. This paper proposes a feasible approach to study the fatigue damage of offshore wind turbines using the in-situ strain data based on a statistical analysis of stress amplitude and cycles. First, the hot-spot stress at the corresponding monitoring locations is calculated using the strain monitoring data from an offshore wind farm in the East China Sea. Second, the stress amplitude and cycles are solved using the rain-flow counting method. Subsequently, the weekly distribution statistics of stress amplitude and cycles are fitted using Weibull distribution. The Chi-square test is used to verify the confidence level of the probability density function of the weekly stress amplitude and cycles. Finally, according to the statistical distribution of stress amplitude and cycles, the cumulative damage is analyzed based on the hot-spot stress *S-N* curve of steel structures with cathodic protection in seawater. The fatigue damage obtained based on the monitored data is roughly consistent with the numerical calculation results. However, the proposed method underestimated the fatigue damage compared to the design results obtained by numerical prediction. Though these fatigue results are not mutually consistent, they can all confirm that the wind turbine would not suffer fatigue issues at present, as the fatigue damages are all below the threshold. Further efforts should be made to handle this inconsistency in fatigue prediction.

Hou Qiao, Key Laboratory of Far-shore Wind Power Technology of Zhejiang Province, POWERCHINA HUADONG Engineering Corporation (HDEC), Hanzhou, China
Guangming Xu, POWERCHINA HUADONG Engineering Corporation (HDEC), Hangzhou, China
Ce Shen, Zhejiang Electric Power Construction Co., Ltd., Ningbo, China
Yonglei Su, Shanghai Xiaomi Intelligent Technology Co, Ltd., Shanghai, China
Wei Li, Key Laboratory of Far-shore Wind Power Technology of Zhejiang Province, POWERCHINA HUADONG Engineering Corporation (HDEC), Hanzhou, China
Chuanrui Guo, College of Civil and Transportation Engineering, Institute of Urban Smart Transportation & Safety Maintenance, Shenzhen University, Shenzhen, China

INTRODUCTION

Offshore wind power is one of the most mature and effective types of offshore renewable energy. However, the external environment where the offshore wind turbines are located includes the coupling effect of wind, wave, ocean current, and complex marine geological conditions, resulting in design difficulties and high costs in offshore wind development. To reduce the cost of offshore wind development, it is necessary to reduce the lifecycle cost as much as possible, the cost of offshore wind turbine construction and maintenance costs are all included. Aiming at optimizing operation and maintenance costs, the fatigue issue of welding parts (tubular joints, etc.) in steel structures is especially critical in offshore wind turbines due to the structural complexity and their harsh environments.

Researchers in civil engineering (bridge structures) have already done some work in the assessment of structural fatigue based on monitoring data. Abdullah et al. (Abdullah et al. 2021) used the Gumbel distribution model combined with strain data to evaluate the reliability of the fatigue life of automotive leaf springs under variable amplitude road load. On-site monitoring data is also analyzed using the empirical mode decomposition (EMD) algorithm and rain flow counting method (Lei et al. 2022) to evaluate the fatigue remaining life of rigid suspension brackets in highway arch bridges. To evaluate the fatigue life of steel bridges, typical time histories of dynamic strain (Li et al. 2003) and universal standard stress spectrum considering different load effects (Ye et al. 2012) were obtained, then the fatigue life of key welding details on the bridge can be evaluated. Low-stress cycles were found to be misleading and should be handled with care. Otherwise, they can lead to inaccurate fatigue life results (Deng et al. 2015). Method to reduce the uncertainty of fatigue life assessment was also discussed (Pasquier et al. 2014). Deep Learning method was also introduced to the fatigue evaluation of experimental beams in the lab (Gulgec et al. 2020). The development history and current status of fatigue assessment for steel bridges and the related methods were also summarized (Ye et al. 2014). However, there is currently relatively little work on fatigue assessment based on measured strain data in offshore engineering (especially offshore wind turbines) worldwide (Hübler and Rolfes 2022; Tarpø et al. 2022).

This paper proposes a feasible approach to study the fatigue damage of offshore wind turbines using the in-situ strain data from an offshore wind farm in Jiangsu, China. The proposed fatigue evaluation method is based on the statistical analysis of stress amplitude and cycles, and the results are far from satisfactory at this moment. However, the method can estimate fatigue damage early in a structural failure, thus avoiding unnecessary damage. Therefore, this paper provides a new perspective to improve the reliability of the whole lifecycle of offshore wind turbines, thus reducing the operation and maintenance costs.

METHODOLOGY AND RESULTS

Wind Turbine Foundation and Related Design Results

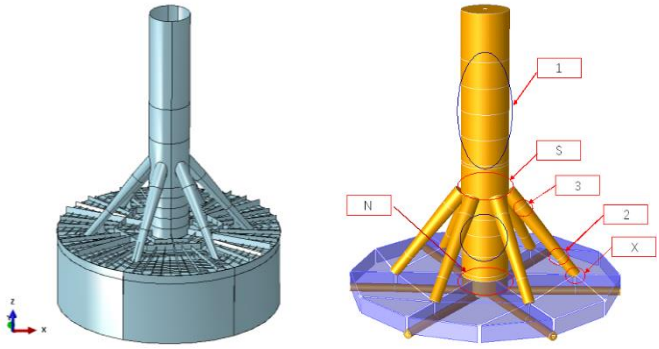

Figure 1. Schematic diagram of steel composite bucket foundation

The foundation type of the offshore wind farm studied is a composite bucket foundation, as shown in Figure 1. The first-order modal frequency of the foundation is f_0 = 0.2176Hz. A finite element model was used to analyze the steel composite foundation. The stress results are shown in Figure 2. As shown, the maximum Mises stress on the foundation is about 256MPa. Meanwhile, it can be seen that the maximum stress is located at the intersection of the support rod and the main beam (see Figure 2).

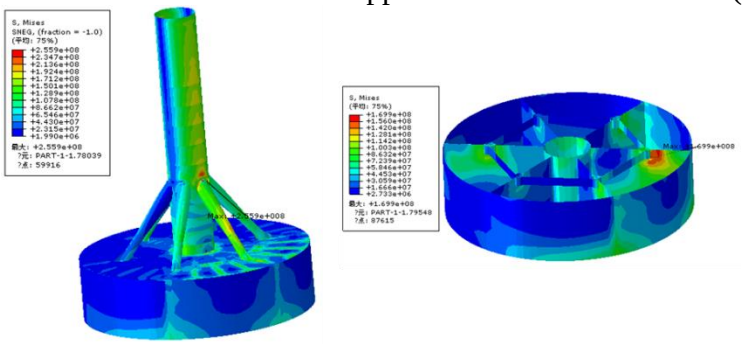

Figure 2. Overall stress distribution of steel composite cylindrical foundation

The fatigue results are presented below. For the intersection node between the support rod and the main beam, the polished *S-N* curve is used, and the total fatigue damage is 0.802, corresponding to a fatigue life of 31.2 years. The remaining weld joints adopt S-N curves without grinding. The fatigue damage is shown in Table 1.

TABLE 1. FATIGUE DAMAGE RESULTS

	Fatigue by wind load	Fatigue by wave load	Total	Fatigue Life
1	0.67	0.01	0.68	36.8
2	0.38	0.025	0.405	61.7
3	0.121	0.005	0.126	198.4
S	0.79	0.012	0.802	31.2
X	0.483	0.024	0.507	49.3
N	0.017	0.000	0.017	1470.6

Strain Sensors and Monitoring Data

Based on the finite element results, the strain monitoring locations for the steel bucket foundation are shown in Figure 3 (left: side view. right: top view). The distribution of strain monitoring sensors is shown in Table 2.

TABLE 2. STRAIN MONITORING POINTS (PW: PREVAILING WIND, PPW: PERPENDICULAR TO PW. N: NORMAL. A: ABNORMAL)

Sensor	1	2	3	4	5	6	7
Direction	PW	PPW	PW	PPW	PW	PW	PW
Status	N	N	A	N	N	A	N

Among the strain sensors, sensors 3 and 6 are damaged and no strain data for the corresponding location exists. On the other hand, sensors 1, 2, 4, 5, and 7 are normal, and there are several strain monitoring data segments from November 2021 to February 2023, with a sampling interval of 5 minutes. The strain measurement range is tensile 1200 $\mu\varepsilon$, compressive 1200 $\mu\varepsilon$, with a resolution of 0.3% F.S. (full scale) as 7.2 $\mu\varepsilon$. Unfortunately, the data is discontinuous, and the total time length for each data segment is different. In addition, some monitoring data recorded temperature data during the same period synchronously.

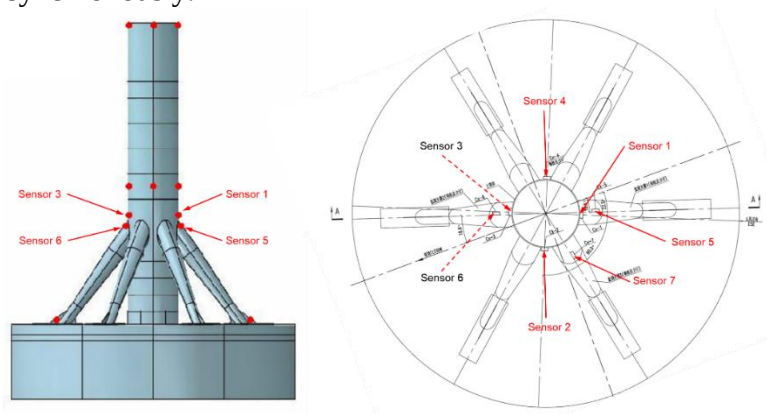

Figure 3. Strain sensors for steel bucket foundation

There are missing values and outliers in the strain data. After data preprocessing and filling of the strain monitoring data, the overall distribution of the strain monitoring data is shown in Figure 4. From the above strain data distribution, it can be seen that the strain data does not exhibit prominent statistical characteristics.

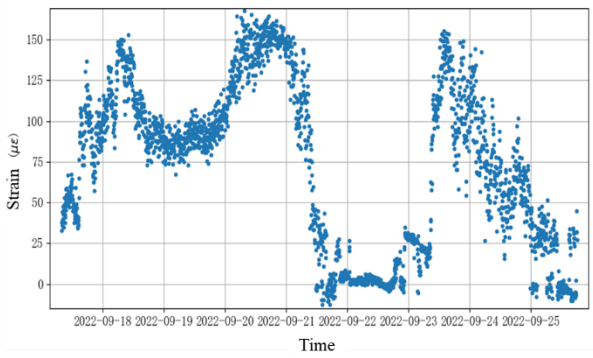

Figure 4. Distribution of strain data (September 2022)

Hot-spot Stress Computation

In the design of offshore wind structures, the hot-spot stress *S-N* curve is usually used for structural damage evaluation. The assessment of fatigue damage is carried out by analyzing the hot-spot stress characteristics.

Assuming that the foundation of the wind turbine is a uniform cross-section beam, the relationship between axial stress σ, bending moment M, and strain is

$$\sigma = \frac{My}{I} = E\varepsilon \quad (1)$$

Where y is the distance from the neutral plane of the beam under bending, and I is the moment of inertia of the beam relative to the centroid axis. On the outer surface of the beam $y = D/2$, D is the outer diameter of the beam. The sign of the axial stress σ needs to be determined based on the sign of strain obtained from monitoring (or the direction of the bending moment). The foundation type of offshore wind turbine may be a monopile, high-pile cap, suction bucket, or jacket type. The stress-strain relationship corresponding to the steel structures can be approximated following the correlation relationship of a uniform cross-section beam, so the nominal stress corresponding to the monitoring locations can be approximated as $\sigma \approx E\varepsilon$.

According to the sensor locations in Figure 3, sensors 1 to 4 are located on the main beam, and sensors 5 to 7 are located on the supporting rod. According to the SCF calculation results, it can be concluded that the SCF of the connection node between the support rod and main beam of the steel bucket foundation is K=1.48 (sensors 5, 6, and 7). The SCF of joints on the main beam is K=1.17 (upper) and 1.09 (lower), corresponding to sensors 1, 2, 3, and 4, respectively. Therefore, the hot-spot stress at the corresponding sensor location is $S = K\sigma$.

S-N Curve of Hot-spot Stress for Offshore Wind Turbines

According to DNV RP-C203, the durability curve of steel is defined as:

$$\log N = \log \bar{a} - m \log S \quad (2)$$

N is the number of stress cycles, S is the stress amplitude, m is the slope parameter, and $\log \bar{a}$ is the intercept of $\log N$ axis. According to the differences in slope parameters and intercept, the DNV RP C203 specification defined the *S-N* curves for different structures and joints.

According to DNV RP C203, the W3 to B1 curves correspond to steel structures with cathodic protection in seawater. Since strain sensors 1 to 7 belong to tubular joints and the corresponding weld seam is unilateral, the T-curve, C-curve, D-curve, or F-curve can be selected. At the same time, referring to design data, the *S-N* curve in API specifications (after this referred to as API curve) can also be used. According to Figure 5, considering the differences in fatigue performance corresponding to different curves, the C, API, and F curves can be selected for fatigue evaluation at the measurement point, corresponding to the minimum and maximum damage that may occur to the structure, respectively.

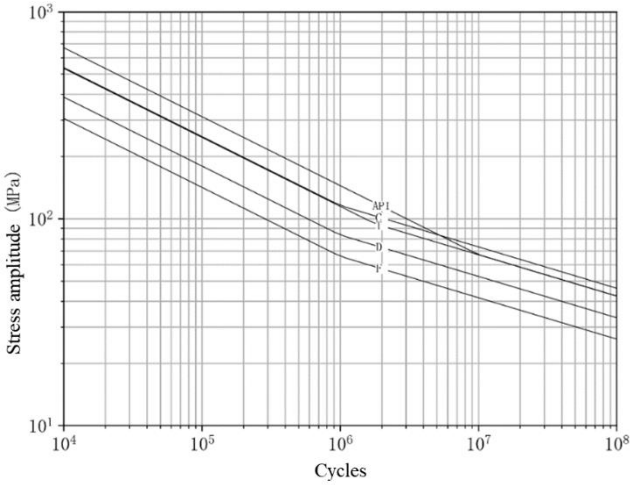

Figure 5. Comparison of S-N curves applicable to strain measurements

The API curve, C curve, and F curve were selected for fatigue assessment, while the intersection point of the two linear segments of the C curve and the F curve is $N_d = 10^6$, and the intersection point of two linear segments of the API curve is $N_d = 10^7$.

As the elastic modulus of DH36 steel commonly used in offshore wind structures in China is 206 GPa, the minimum stress that can be obtained is estimated as 2.19 MPa considering that the strain gauge resolution is 7.2 $\mu\varepsilon$. However, due to the limitation on sensor resolution, the stress values obtained below 2.19 MPa have no practical significance, and these values are modified to 2.19MPa.

Statistical Characteristics of Stress Amplitude and Cycles

Some previous studies have shown that high-stress cycling under variable amplitude cyclic loading can affect the fatigue damage behavior of small stress amplitudes below the fatigue limit. Therefore, the fatigue damage of small stress amplitude cyclic loading below the fatigue limit cannot be ignored, which can be made up of extensive stress cycles.

Considering the large cycles under small load amplitudes, it is recommended to reduce the number of cycles under the fatigue limit by a reduction factor according to BS 5400, which is defined as

$$\lambda_i = \begin{cases} (S_i/S_0)^2 & S_i < S_0 \\ 1 & S_i > S_0 \end{cases}$$

Where S_0 and S_i are the fatigue limit and the stress amplitude, respectively. When the fatigue endurance limit is set to $N = 10^7$, the fatigue limit S_0 of the C curve corresponds to=73.10 MPa, the D curve corresponds to=52.63 MPa, and the T curve corresponds to=67.09 MPa.

The statistical characteristics of stress amplitude and number of cycles are analyzed in the following. Based on the overall distribution and confidence level of stress amplitude and cycles in the monitoring data, the typical distribution parameters are used to estimate the fatigue damage at each location.

The distribution of stress amplitude and cycles are shown in Figure 6. According to the rain flow counting method, daily statistics may highlight the influence of small stress

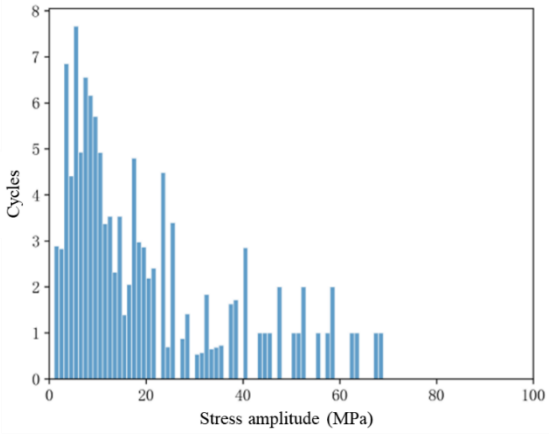

Figure 6. Distribution of weekly stress amplitude and cycles

amplitude segments. Conversely, weekly statistics may emphasize the influence of more significant stress amplitude segments in the data. In the calculations, we found that the two statistical methods have little impact on the distribution of stress statistics, though there are certain differences in stress amplitude and cycles when the stress amplitude is small. Therefore, only weekly statistics are used in the following analysis.

The following describes the statistical feature estimation procedure for stress amplitude and cycles. According to Figure 6, the Weibull distribution or normal distribution is assumed, and hypothesis testing is performed. Since the occurrence probability of abnormal data with a small significance level is smaller, the distribution with a small significance level is considered as the obtained distribution form.

Statistical Distribution of Hot-spot Stress

The Weibull distribution commonly used in engineering includes three-parameter distribution and two-parameter distribution forms. The probability density function of the three-parameter Weibull distribution is

$$f(x;\lambda,k,\gamma)=\begin{cases}\frac{k}{\lambda}\left(\frac{x-\gamma}{\lambda}\right)^{k-1}e^{-\left(\frac{x-\gamma}{\lambda}\right)^{k}} & ,\ x\geq 0\\ 0 & ,\ x<0\end{cases} \tag{3}$$

Where the scale parameter $\lambda \geqslant 0$, the shape parameter $k \geqslant 0$, the position parameter γ is unrestricted, and the function is defined at $x \geqslant \gamma$ (0 when x<γ). The probability density function of the two-parameter Weibull distribution is

$$f(x;\lambda,k)=\begin{cases}\frac{k}{\lambda}\left(\frac{x}{\lambda}\right)^{k-1}e^{-\left(\frac{x}{\lambda}\right)^{k}} & ,\ x\geq 0\\ 0 & ,\ x<0\end{cases} \tag{4}$$

Where the scale parameter $\lambda \geqslant 0$, the shape parameter $k \geqslant 0$, and the function definition domain is $x \geqslant 0$.

Using the least square method, different numbers of weekly data were selected to fit the Weibull distribution parameters. The fitting results are shown in Figure 7, where the enlarged image of the red area A is shown on the right. As shown, the fitted curves have significant differences when using 5-9 weeks of data. However, when weekly data of 10 weeks or more are used, there is no significant difference in the fitting curves of the stress amplitude and cycles. Therefore, weekly monitoring data consisting of 12 weeks are used to fit the distribution characteristics of stress amplitude and cycles.

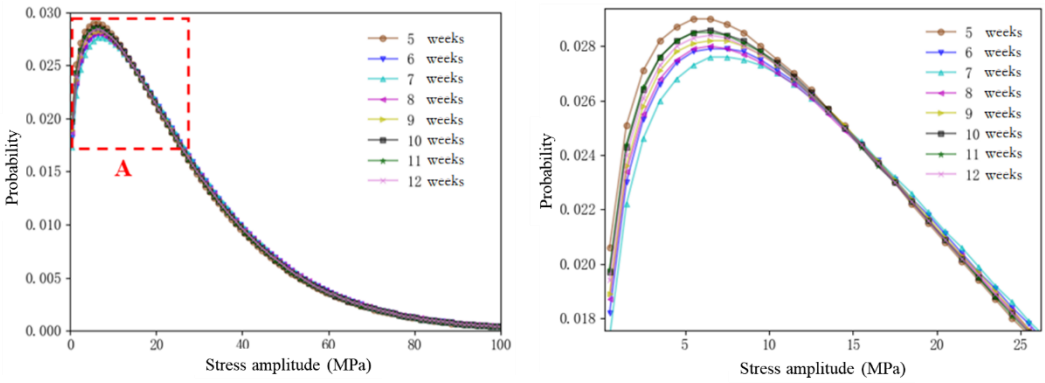

Figure 7. Fitting results of the probability distribution (A: local view)

Using monitoring data from 12 weeks for weekly distribution fitting, the parameters of the three-parameter distribution are λ=24.9777, k=1.3036, and γ=0.128284, while the parameters of the two-parameter Weibull distribution are λ=25.13, k=1.31223.

To verify the Goodness of fit, the COD (Coefficient of Determination) R^2 of the two distributions is used, which is the proportion of the variation in the dependent variable that is predictable from the independent variable.

$$R^2 = 1 - \frac{\sum_i (y_i - f_i)^2}{\sum_i (y_i - \bar{y})^2}, \quad \bar{y} = \frac{1}{n}\sum_i^n y_i \tag{5}$$

Where y_i is the i-th value of the data, $\bar{y}$ is the mean value, f_i is the fitted value of the i-th data, and n is the number of samples. R^2 ranges from 0 to 1, representing the percentage of the square of the correlation between the predicted and actual values of the target variable. An R^2 value close to 1 indicates high credibility in the model-fitting results. For example, the R^2 of the three-parameter Weibull distribution is 0.997558, and the R^2 of the two-parameter Weibull distribution is 0.997556. The R^2 values of both fitting models are close to 1, indicating that the model fits well.

Considering that there is little difference between the two kinds of Weibull distribution, a two-parameter Weibull distribution model is proposed to describe the probability distribution of the stress amplitude and cycles. The obtained probability density function of cycles concerning stress amplitude is as follows

$$f_N(S) = 0.052218\left(\frac{S}{25.13}\right)^{0.31223} \mathrm{e}^{-\left(\frac{S}{25.13}\right)^{1.31223}} \tag{6}$$

The fitting results of the two-parameter Weibull distribution are shown in Figure 8.

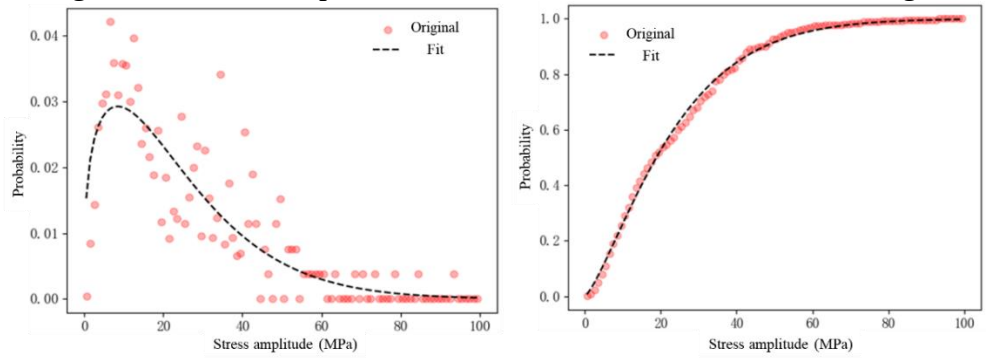

Figure 8. Fitting results of the cumulative probability distribution

The Chi-square test is used to verify the confidence level of the probability density function of the weekly stress amplitude and cycles. It is shown in the Chi-square test

that when the unknown distribution follows a specific probability distribution, the statistics χ^2 should satisfy $\chi^2(k-r-1)$

$$\chi^2 = \sum_{i=1}^{k} \frac{f_i^2}{n\hat{p}_i} - n \sim \chi^2(k-r-1) \tag{7}$$

If $\chi^2 < \chi_\alpha^2(k-r-1)$, the monitoring data follows the given probability distribution at the significance level α.

Assuming that the stress statistics follow the above two-parameter Weibull distribution, *r*=2, the stress amplitude sample can be divided into *k*=6 non-intersecting subsets (no less than five required by the Chi-square test). When the monitoring data is substituted into the distribution function, we can obtain the following results in Table 3.

TABLE 3. CHI-SQUARE TEST TABLE

S	**(0,10)**	**[10,20)**	**[20,30)**	**[30,40)**	**[40,50)**	**[50,100)**
f_i	10	10	10	10	24	8
A_i	A_1	A_2	A_3	A_4	A_5	A_6
$\hat{p}_i$	0.2580	0.2654	0.1934	0.1244	0.0739	0.0849
$f_i^2/(n\hat{p}_i)$	3.8756	3.7681	5.1703	8.0377	77.9695	7.5393

Based on the above results, it can be seen that,

$$\chi^2 = \sum_{i=1}^{k} \frac{f_i^2}{n\hat{p}_i} - n = 106.3605 - 480 = 6.3605 < \chi_{0.05}^2(3) = 7.815$$

Therefore, the monitored data follows the proposed two-parameter Weibull distribution at the significance level $\alpha = 0.05$. This means that the monitoring data follows the above two-parameter Weibull distribution, the probability of abnormal (non-Weibull) data occurrence is not higher than 5%, and the confidence level of the monitoring data following a two-parameter Weibull distribution is not less than $1 - \alpha = 95\%$.

Fatigue Evaluation using the Distribution of Stress Amplitude and Cycles

Subsequently, the fatigue damage of offshore wind turbines is directly calculated based on the hot-spot stress *S*-*N* curve. The results are susceptible to distribution parameters, and further investigations are in progress to improve its reliability. Here, we just present a first proof of concept and briefly verify the results.

According to the design results, the required first-order modal frequency of the bucket foundation is f_0 = 0.2176Hz. Therefore, its natural vibration period is T_0 = 4.5956s. As the modal frequency for a typical wind turbine should always be larger than the required frequency value otherwise fault or shutdown would occur, the maximum number of cycles per week is

$$N_{\text{all}} = \frac{T}{T_0} = 131604.4780 \tag{8}$$

Where *T* is the total time duration in a week, *T* = 604800 seconds.

According to the probability density function of the distribution of the weekly stress amplitude and cycles in Equation (6), the number of stress cycles under the stress amplitude level *S* is *N*(*S*), which is

$$N(S) = N_{\text{all}} \times f_N(S) \tag{9}$$

Considering that the hot-spot stress *S-N* curve with cathodic protection in the seawater used is bilinear, the fatigue damage calculation is carried out in two steps concerning the stress amplitudes separated by the intersection of two linear segments of the *S-N* curve. The stress amplitude at the intersection of two segments satisfies

$$\log S_d = \frac{1}{m}\log \bar{a} - \log N_d \tag{10}$$

Where the corresponding number of cycles N_d=1×10^6, therefore S_d = 65.8163 MPa.

In the first stress range where the stress amplitude S is less than S_d, the parameter of the *S-N* curve is $m_1, \log_{10}\bar{a}_1$. According to the probability density function in Equation (6), numerical integration is performed to solve the fatigue damage in the range 0 ~ S_d

$$D_1 = \int_0^{S_d} \frac{N(S)}{N_1} \mathrm{d}S \tag{11}$$

Where N_1 is the cycle number (life) corresponding to the stress amplitude S

$$N_1 = 10^{\log_{10}\bar{a}_1 - m_1 \log_{10} S} \tag{12}$$

In the second stress range where the stress amplitude is greater than S_d, the parameter of the *S-N* curve is $m_2, \log_{10}\bar{a}_2$. According to the probability density function in Equation (6), numerical integration is performed for the fatigue damage in the range $S > S_d$

$$D_2 = \int_{S_d}^{+\infty} \frac{N(S)}{N_2} \mathrm{d}S \tag{13}$$

Where N_2 is the cycle number (life) corresponding to the stress amplitude S

$$N_2 = 10^{\log_{10}\bar{a}_2 - m_2 \log_{10} S} \tag{14}$$

TABLE 4. COMPARISON OF FATIGUE RESULTS

	Sensor 5	Numerical Result
Fatigue damage (25 years)	0.540	0.802
Fatigue life (year)	46.30	31.20

According to Equations (11) ~ (14), the fatigue damage of sensor 5 can be solved, as shown in Table 4. The fatigue damage obtained by the monitoring data is slightly smaller than the numerical result (about -32.67%), leading to a longer fatigue life than the numerical one (about +48.40%). Therefore, it can be concluded that the proposed method underestimated the fatigue damage compared with the design results obtained by numerical prediction. The difference happens due to several factors.

First, the proposed method is highly dependent on the proposed statistical distribution fitted using the obtained stress amplitude and cycles. Besides, though the in-situ strain monitoring is designed and installed carefully, the obtained results can still be contaminated with data noise and thus be erroneous. Inappropriate distribution of stress amplitude and cycles used, or bad strain data, can all lead to untrustworthy fatigue results.

Second, the fatigue results obtained by the numerical method are obtained using the statistical design input, which is always considered with a return period of 50 years in China. The monitoring data may never present a result that complies with the statistical characteristics.

However, all the results confirm that the wind turbine would not suffer fatigue issues at present as the fatigue damages are all below the threshold, though the results are not mutually consistent. Further efforts should be made to handle this inconsistency in fatigue prediction.

CONCLUSIONS

To optimize offshore wind turbines' operation and maintenance costs, this paper proposes a feasible approach to study fatigue damage using the in-situ strain data from an offshore wind farm in China. The proposed fatigue evaluation method is based on the statistical analysis of stress amplitude and cycles, which were fitted using the Weibull distribution. The Chi-square test is used to verify the confidence level of the probability density function of the weekly stress amplitude and cycles. According to the statistical distribution of stress amplitude and cycles, the cumulative damage is analyzed based on the hot-spot stress *S-N* curve of steel structures containing cathodic protection in seawater. The fatigue damage obtained based on the monitored data is roughly consistent with the numerical calculation results. However, the proposed method underestimated the fatigue damage compared to the design results obtained by numerical prediction. Though these fatigue results are not mutually consistent, they can all confirm that the wind turbine would not suffer fatigue issues as the fatigue damages are all below the threshold. Further efforts should be made to handle this inconsistency in fatigue prediction. The fatigue results obtained from in-situ monitoring data are far from satisfactory at this moment, and further efforts should be made to handle the inconsistency in fatigue prediction. However, the method can estimate fatigue damage early in a structural failure, thus avoiding unnecessary damage. Therefore, this paper provides a new perspective to improve the reliability of the whole lifecycle of offshore wind turbines, thus reducing the operation and maintenance costs.

REFERENCES

1. Abdullah, L., S. S. K. Singh, S. Abdullah, A. H. Azman, and A. K. Ariffin. 2021. “Fatigue reliability and hazard assessment of road load strain data for determining the fatigue life characteristics.” Engineering Failure Analysis, 123: 105314.
2. Deng, Y., Y. Liu, D.-M. Feng, and A.-Q. Li. 2015. “Investigation of fatigue performance of welded details in long-span steel bridges using long-term monitoring strain data.” Struct. Control Health Monit., 22 (11): 1343–1358.
3. Gulgec, N. S., M. Takáč, and S. N. Pakzad. 2020. “Structural sensing with deep learning: Strain estimation from acceleration data for fatigue assessment.” Computer-Aided Civil and Infrastructure Engineering, 35 (12): 1349–1364.
4. Hübler, C., and R. Rolfes. 2022. “Probabilistic temporal extrapolation of fatigue damage of offshore wind turbine substructures based on strain measurements.” Wind Energy Science, 7 (5): 1919–1940. Copernicus GmbH.
5. Lei, J., Q. Kong, X. Wang, and K. Zhan. 2022. “Strain monitoring-based fatigue assessment and remaining life prediction of stiff hangers in highway arch bridge.” Symmetry, 14 (12): 2501.
6. Li, Z. X., T. H. T. Chan, and R. Zheng. 2003. “Statistical analysis of online strain response and its application in fatigue assessment of a long-span steel bridge.” Engineering Structures, 25 (14): 1731–1741.
7. Pasquier, R., J.-A. Goulet, C. Acevedo, and I. F. C. Smith. 2014. “Improving fatigue evaluations of structures using in-service behavior measurement data.” J. Bridge Eng., 19 (11): 04014045.
8. Tarpø, M., S. Amador, E. Katsanos, M. Skog, J. Gjødvad, and R. Brincker. 2022. “Data-driven virtual sensing and dynamic strain estimation for fatigue analysis of offshore wind turbine using principal component analysis.” Wind Energy, 25 (3): 505–516.
9. Ye, X. W., Y. Q. Ni, K. Y. Wong, and J. M. Ko. 2012. “Statistical analysis of stress spectra for fatigue life assessment of steel bridges with structural health monitoring data.” Engineering Structures, 45: 166–176.
10. Ye, X. W., Y. H. Su, and J. P. Han. 2014. “A state-of-the-art review on fatigue life assessment of steel bridges.” Mathematical Problems in Engineering, 2014: 1–13.